Synchronization regimes in coupled noisy excitable systems

Bambi Hu[1,2] and Changsong Zhou[1]
[1]*Department of Physics and Center for Nonlinear Studies, Hong Kong Baptist University, Hong Kong, China*
[2]*Department of Physics, University of Houston, Houston, Texas 77204*
(Received 30 May 2000; published 10 January 2001)

We study synchronization regimes in a system of two coupled noisy excitable systems which exhibit excitability close to an Andronov bifurcation. The uncoupled system possesses three fixed points: a node, a saddle, and an unstable focus. We demonstrate that with an increase of coupling strength the system undergoes transitions from a desynchronous state to a *train synchronization* regime to a phase synchronization regime, and then to a complete synchronization regime. Train synchronization is a consequence of the existence of a saddle in the phase space. The mechanism of transitions in coupled noisy excitable systems is different from that in coupled phase-coherent chaotic systems.

DOI: 10.1103/PhysRevE.63.026201 PACS number(s): 05.45.−a, 05.40.−a

I. INTRODUCTION

The study of coupled oscillators is one of the fundamental problems with applications in various fields [1]. Mutual synchronization is of great interest and importance among the collective dynamics of the coupled oscillators. The notation of synchronization has been extended to include a variety of phenomena in the context of interacting chaotic oscillators, such as complete synchronization [2], generalized synchronization [3], phase synchronization [4], and lag synchronization [5]. Transitions from phase to lag to complete synchronization have been demonstrated in a system of two coupled nonidentical Rössler chaotic systems [5] which are phase coherent.

Synchronization has also been studied in noise-induced motions. It was found that the stochastic processes in coupled stochastic bistable systems become coherent when the coupling strength exceeds some critical value [6]. The mean switching frequency in stochastic bistable systems can be locked by an external period force [7]. Stochastic resonance can be understood from the view point of enhanced frequency locking and phase synchronization of the noise-induced motion to the external signal [8]. Due to this synchronization, coupled stochastic bistable elements can display global synchronization to an external periodic signal, which has the effect of enhancing the stochastic resonance in the array [9]. Pure noise can induce coherence resonance in some excitable systems [10–12]. Phase synchronization has been demonstrated in systems of two coupled coherence resonance oscillators [13]. Global synchronization [14,15] and array-enhanced coherence resonance [15] have been observed in extended excitable media. Recently, synchronization of noisy oscillatory models found an interesting application in the oscillatory zoning of minerals [16].

However, whether different synchronization regimes similar to those in coupled phase-coherent chaotic systems also exist in coupled stochastic systems are not clear. Here we study this problem in a system of two coupled noisy excitable systems close in parameter space to an Andronov homoclinic bifurcation [17]. This bifurcation is a quite general mechanism for excitability observed in many laser [18] and biological [11] systems. Typically, three equilibria—a stable node (N), a saddle (S), and an unstable focus (F)—coexist in the uncoupled system. The unstable manifold of the saddle approaches the node, and the saddle is connected to the focus by its stable manifold (Fig. 1, region II). In the presence of noise, the fixed state at the node may be kicked over the separatrix of the stable manifold, and the system will only come back to the node after a large excursion following the guidance of the unstable manifold, displaying a spike in the neuronal systems or a dropout event (low-frequency fluctuation) in laser systems [18].

We demonstrate that, with an increase of the coupling strength, one generally observes phase synchronization and complete synchronization regimes. In the system, transition between different regimes is blurred due to the stochastic nature of the dynamics. A synchronization regime, *train synchronization*, is found prior to the phase synchronization region, in which the two systems exhibit phase synchronization of spike trains, while the number of pulses in the spike trains may be different for the two coupled noisy oscillators. This behavior occurs when the trajectories cross the stable manifold of the saddle before coming back to the node, and is thus universal in excitable systems close to the Andronov bifurcation. The mechanism of the transitions in this type of

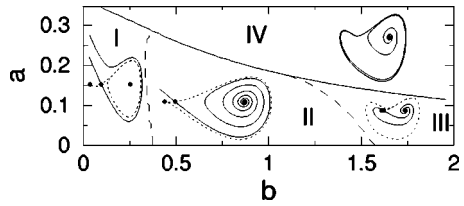

FIG. 1. Bifurcation diagram and phase portraits. In regions I, II and III, a node, a saddle and an unstable focus coexist. In region IV, the node and the saddle disappear via a saddle-node bifurcation. In regions I and III, there are two stable attractors, the node and a limit cycle. The limit cycle disappears via the Andronov homoclinic bifurcation (dashed lines), and the node becomes the global attractor in region II where the system behaves as an excitable one. Close to the homoclinic bifurcation point, the stable and unstable manifolds (solid line and dotted line in the phase portraits) of the saddle are close to each other.

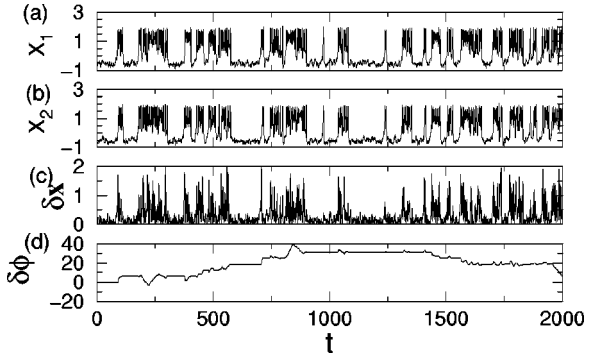

FIG. 2. An example of train synchronization for $g=0.16$. (a) and (b) are spikes of the two systems, and (c) is the synchronization error $\delta x=|x_1-x_2|$. (d) is the phase difference between the spikes.

system is different from that in coupled phase-coherent chaotic systems.

II. SYSTEM AND RESULTS

It is a typical strategy in nonlinear dynamics to study paradigmatic models whose solutions possess desired features. We study synchronization phenomena in a simple model with the above desired phase space structure. It reads

$$\dot{x}_1=y_1+g(x_2-x_1)+\sqrt{\sigma}\xi_1, \tag{1}$$

$$\dot{y}_1=x_1-y_1+x_1y_1-x_1^3+bx_1^2+a_1, \tag{2}$$

$$\dot{x}_2=y_2+g(x_1-x_2)+\sqrt{\sigma}\xi_2, \tag{3}$$

$$\dot{y}_2=x_2-y_2+x_2y_2-x_2^3+bx_2^2+a_2. \tag{4}$$

This simple mathematical model, although not derived from a specific physical process, gives a good account of the interspike time distributions of low-frequency fluctuations in a laser system [19], which suggests that the underlying mechanism of the low-frequency fluctuation are excitability and noise.

In our investigation, the two oscillators are assumed to be nonidentical, e.g., $a_1\neq a_2$. Similar behaviors, however, are observed for identical systems. The noises ξ_1 and ξ_2 are independent Gaussian white ones with a variance 1.0.

Figure 1 depicts the phase diagram in a parameter space (b,a) for the uncoupled element. In the following, we take $a_1=0.25$, $a_2=0.23$, $b=0.4$, and $\sigma=0.01$, in the excitable region II, and study the synchronization behavior with an increase of coupling strength g. $b=0.4$ is close to the homoclinic bifurcation between regions I and II.

In the coupled excitable systems, noise-induced spikes in one system may excite another system due to coupling. When g is rather small, this coupling-induced excitation may not always occur, and the systems are in desynchronization regime. As g increases to large enough values, a noise-induced spike can almost always excite the other system. This excitation may produce a train of spikes in the systems before they come back to the quiescent states at the nodes. A typical behavior is shown in Fig. 2, where the two systems

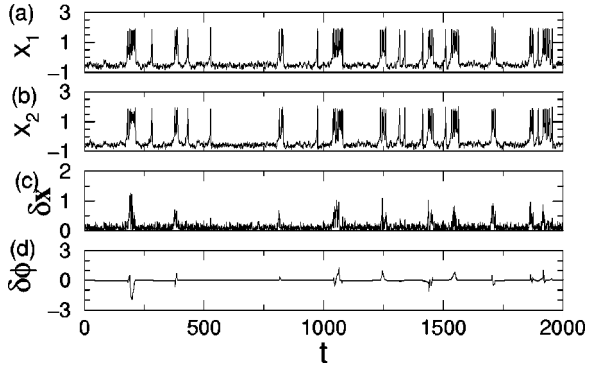

FIG. 3. An example of phase synchronization for $g=0.34$. The caption is the same as in Fig. 2.

display synchronization in a ''train'' fashion, while the numbers of spikes within the synchronized spike trains can be different for the two subsystems, as seen by the phase slips (defined below) in Fig. 2(d). The spiking frequencies are different in the two subsystems, and the synchronization errors are rather large during the spiking period of the systems. With a further increase of g, the two subsystems come into the phase synchronization regime where the spike frequencies become identical; however, the errors between phase synchronized spikes of the two subsystems are still relatively large, as seen in Fig. 3, because there are appreciable phase differences between the spikes, although there are no phase slips ($|\delta\phi|<2\pi$). Finally, for large enough g, the phase differences between the two subsystems become rather small, and the difference $|x_1-x_2|$ reaches the noise level, achieving complete synchronization, as illustrated in Fig. 4. One also notes that the average number of pulses in the spike trains decreases with increasing coupling strength.

To characterize synchronization transitions and *train synchronization* in the system, we first define a train of spikes by threshold testing: let τ_k be the time at which the system produces the kth spike determined in numerical simulations when the variable x crosses over x_F from below. x_F is the x value of the unstable focus F. Two successive spikes are considered to be in the same train if the spike interval $\tau_{k+1}-\tau_k<T_{th}$. T_{th} is a prescribed value for the threshold testing. The typical behavior of this system is not sensitive to this value. In this way, we can determine the firing moment τ_i^c of

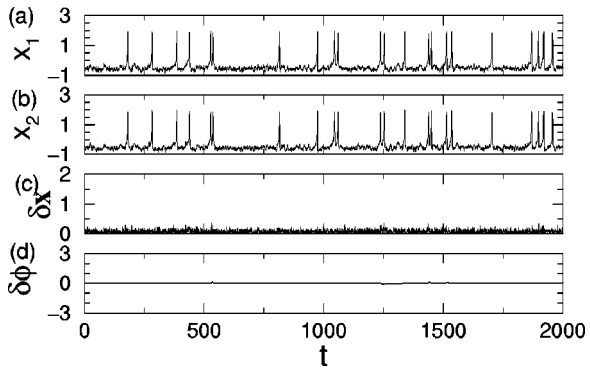

FIG. 4. An example of complete synchronization for $g=0.70$. The caption is the same as in Fig. 2.

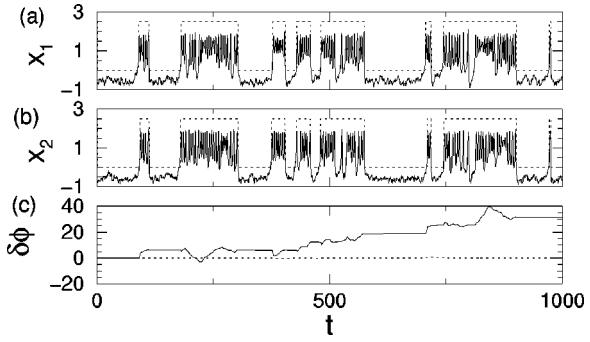

FIG. 5. An example of train synchronization for $g=0.16$ and $T_{th}=20$. (a) and (b) are spikes (x, solid line) and spike trains (x^c, dotted line) of the two systems. (c) Phase differences of the spikes (solid line) and the spike train (dotted line).

the ith *spike train*. Moreover, we can transfer the spike trains into a binary stream $x^c(t)$. Now we can compute the phase of the spikes and spike trains as

$$\phi(t)=2\pi k+\frac{t-\tau_k}{\tau_{k+1}-\tau_k},\quad \phi^c(t)=2\pi i+\frac{t-\tau_i^c}{\tau_{i+1}^c-\tau_i^c}. \quad (5)$$

For the example in Fig. 2, the spikes are sorted into spike trains by the above threshold testing with $T_{th}=20$, as indicated by the dotted lines in Figs. 5(a) and 5(b). Figure 5(c) depicts the phase differences $\delta\phi=\phi_1-\phi_2$ between the spikes and $\delta\phi^c=\phi_1^c-\phi_2^c$ between the spike trains. It is clearly seen that phase slips occur between the spikes of the two subsystems, while the spike trains are in the phase synchronization state. Thus we call the behavior *train synchronization*.

To quantify the phase slips of the spikes and spike trains, we calculate the phase diffusion constants

$$D=\lim_{t\to\infty}\frac{1}{2t}\langle(\delta\phi-\langle\delta\phi\rangle)^2\rangle,\quad D^c=\lim_{t\to\infty}\frac{1}{2t}\langle(\delta\phi^c-\langle\delta\phi^c\rangle)^2\rangle. \quad (6)$$

For further characterization of the synchronization behavior, we compute the normalized synchronization error S between x_1 and x_2, and S^c between x_1^c and x_2^c (with mean values being dropped) [5],

$$S=\frac{\langle(x_1-x_2)^2\rangle_t}{[\langle x_1^2\rangle_t\langle x_2^2\rangle_t]^{1/2}},\quad S^c=\frac{\langle(x_1^c-x_2^c)^2\rangle_t}{[\langle(x_1^c)^2\rangle_t\langle(x_2^c)^2\rangle_t]^{1/2}}, \quad (7)$$

where $\langle\,\rangle_t$ denotes an average over time. We also compute the relative maximal synchronization error

$$R=\frac{\langle\max(|x_1-x_2|)\rangle}{[\langle\max(x_1)\rangle\langle\max(x_2)\rangle]^{1/2}}, \quad (8)$$

where $\max(\cdot)$ is the maximum of a variable in a period of long enough time, and $\langle\cdot\rangle$ denotes an ensemble average. R measures the ratio of the maximal synchronization error to the maximal value of the spikes in the subsystems.

These quantities as functions of g with the above system parameters and $T_{th}=20$ are shown in Fig. 6. Figure 6(a)

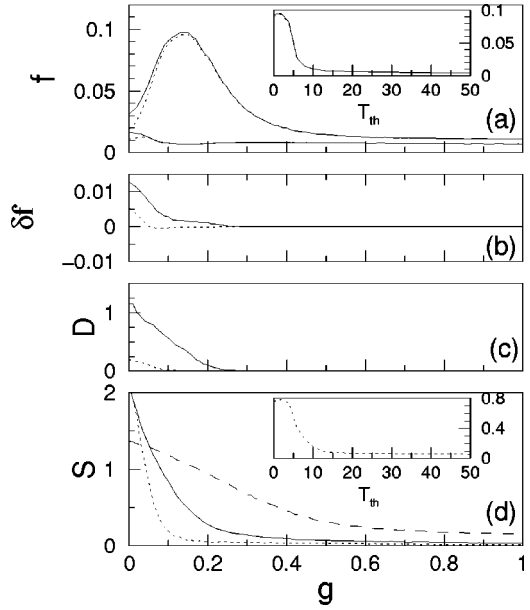

FIG. 6. Illustration of synchronization regimes. (a) Frequencies of the spikes (upper plots) and the spike trains (lower plots) in the two subsystems. (b) Frequency differences and (c) phase diffusion constants of the spikes and the spike trains (dotted lines). (d) Synchronization error S of the spikes (solid line), synchronization error S^c of the spike trains (dotted line), and relative maximal synchronization error R of the spikes (dashed line). The insets in (a) and (d) are the frequency and the synchronization error S^c of the spike trains as a function of T_{th} at $g=0.16$, respectively.

shows the frequencies of the spikes (upper plots) and spike trains (lower plots) of the two systems. In a large range of g, the spike frequencies are higher than those of the uncoupled systems due to the mutual excitations. The frequency differences are shown in Fig. 6(b), and the phase diffusion constants in Fig. 6(c). It is seen that, proceeding to the transition to the phase synchronization regime at about $g=0.3$, there exists a transition to train synchronization at about $g=0.1$. In the train synchronization regime $0.1<g<0.3$, the frequency difference of the spike train is very close to zero, while that of the spikes is not; D^c is very close to zero, but D is not; and S^c is quite small, while S and R are relatively large. After the transition to the phase synchronization regime, the two systems keep in step to produce spikes, but there are appreciable phase differences between the spikes. As a result, the relative maximal synchronization error R is still quite large although the normalized synchronization error S is rather small because large synchronization errors only occur sparsely during the spiking period [Fig. 3(c)]. A further increase of g will reduce the phase differences, and the system moves into complete synchronization regime (about $g>0.6$) where the synchronization errors mainly result from the independent noises in the two subsystems. Since the systems are in a noisy environment, the transitions between different synchronization regimes are not sharp. The behavior of the spike train described in the above is not sensitive to the choice of the threshold T_{th} as long as it is large enough, as shown by the insets in Figs. 6(a) and 6(d), illustrating the saturation property of the frequencies and the synchroniza-

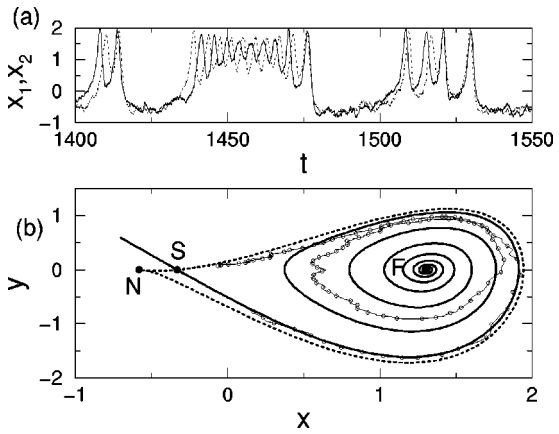

FIG. 7. Mechanism of train synchronization. $g=0.16$. (a) Segments of the time series of the two systems, illustrating phase lags of the spikes. (b) Phase space illustration of early-triggered spikes. The initially lagged noisy trajectory (cycles) is drawn across the stable manifold (solid line), and cycles the unstable focus F before coming back to the node N along the unstable manifold (dotted line).

tion error S^c of the spike trains as functions of T_{th}.

We also note that the spike frequency in the complete synchronization region approaches a value smaller than the values in uncoupled subsystems. Taking into account the small differences between (x_1,y_1) and (x_2,y_2), and denoting $(X,Y)=[(x_1+x_2)/2,(y_1+y_2)/2]$ and $A=(a_1+a_2)/2$, from Eqs. (1)–(4) one obtains the approximation for the average dynamics (X,Y):

$$\dot{X}=Y+\sqrt{\sigma/2}\xi, \tag{9}$$

$$\dot{Y}=X-Y+XY-X^3+bX^2+A. \tag{10}$$

In this approximation, high orders of the differences $(x_i-X,y_i-Y)(i=1,2)$ are ignored. The summation of the two independent noise $\sqrt{\sigma}[(\xi_1+\xi_2)/2]$ results in another noise $\sqrt{\sigma/2}\xi$ which has half of the variance σ. Now it is seen that the two synchronized subsystems act as a single element but are subjected to a weaker noise, so that they have a smaller spiking frequency. A similar behavior was observed in other excitable systems [15]. This property in the complete synchronization region is different from coupled chaotic systems, where the dynamics of the two synchronized systems is restricted to the chaotic attractor in the subspace of a single uncoupled system.

The mechanism of the behavior of train synchronization lies in the crossing of the noisy trajectories over the stable manifold of the saddle before reaching the node. When g is large enough, a noise-induced spike in one system excites the other, but the latter has a pronounced phase lag [Fig. 7(a)]. Close to the Andronov bifurcation, the stable and unstable manifolds are close to each other, a property universal in this type of system. The lagged system is very likely to be drawn across the stable manifold, resulting in an early-triggered spike before reaching the node [Fig. 7(b)]. Moreover, both systems may cross the stable manifold for several times, producing a train of early-triggered spikes. Due to the presence of a saddle point, the flow closer to the saddle is slower. After a few spikes following larger (slower) or smaller (quicker) loops cycling the focus F, the two subsystems adjust their phase difference to a small enough value $[\mathrm{mod}\,2\pi]$ so that both of them can follow the guidance of the unstable manifold to the node, completing a synchronized train of spikes. During the adjustment of the phase difference, one subsystem may cycle the focus a few more loops than the other, resulting in phase slips of the spikes shown in Fig. 5(c). Since phase lags fluctuate and the noises may help or resist the early crossing over the stable manifold, the number of spikes in the spike trains fluctuates. The average number of spikes in one train decreases with increasing g, because the average initial phase lags decrease with an increase of g. This smaller initial phase lags make the systems more likely to follow the guidance of the unstable manifold, and come back to the node together without early return; this can be seen from Figs. 2–4. Also, small enough initial phase lags make the two subsystems follow each other closely enough to produce the same number of spikes in the train, and the system moves into the phase synchronization regime. In the complete synchronization regime, a train of spikes occurs when noise kicks one system across the stable manifold at some point before reaching the node, and the other follows immediately almost without phase lag. Due to the weaker level of the effective noise in Eqs. (9)–(10), an early-triggered spike rarely occurs.

Similar synchronization transitions and train synchronization have been observed for other parameters in the excitable region II. Generally, the distance between the stable and unstable manifolds increases as the system parameters move away from the Andronov bifurcation, and a single spike without early return prevails over spike trains with more than one spike.

Synchronization transitions in coupled excitable system differ in mechanism from those in coupled periodic or phase-coherent chaotic oscillators [5]. In the latter systems, phase synchronization can be described in the weak-coupling limit by a phase model $\delta\dot{\phi}=\delta\omega+2g\sin(\delta\phi)+\delta F$, where $\delta\omega$, the difference of the natural frequencies, and δF, the effect of the amplitude difference, both vanish when the systems approach identity, and the critical value of g for the phase synchronization approaches zero (Arnold tongue) [4]. Lag synchronizations where the states of two oscillators are nearly identical but one system lags in time behind the other, exists between phase synchronization and complete synchronization regimes in some chaotic systems with coherent phases and well-defined frequencies [5]. For coupled excitable systems, phase synchronization can occur only after the coupling is strong enough to induce mutual excitation due to the threshold property of the excitable system, even though the two subsystems are identical. For this reason, the typical behavior does not depend on whether the systems are identical or nonidentical. Due to the noisy environment, the phase lags between the spikes of the two subsystems fluctuate, and one subsystem can advance or lag behind the other for different spikes. There does not exist a well-defined time lag between the systems, and thus there is not a pronounced

lag synchronization regime. Also, transitions between different regimes are blurred due to the stochastic nature of the system.

III. DISCUSSION

In summary, we have demonstrated a series of synchronization transitions in a system of two coupled noisy excitable systems displaying excitability close to the Andronov homoclinic bifurcation. Synchronization in coupled excitable systems only occurs when the coupling is large enough to induce mutual excitation. The initial phase lag between the excited and exciting spikes plays a crucial role in the system behavior. With the phase lags decreasing for larger coupling strengths, the system undergoes transitions from weaker to stronger synchronization regimes. Based on this understanding of synchronization behavior in excitable systems, transitions from desynchronization to phase synchronization and then to complete synchronization can be generally observed in systems of two coupled excitable elements, while train synchronization can be observed in systems close to the Andronov homoclinic bifurcation where stable and unstable manifolds of the saddle are close. The mechanism of synchronization in this type of system is different from that in coupled phase-coherent chaotic systems.

The existence of a saddle in the system has interesting effects on its behavior. Prior to the Andronov bifurcation, the saddle has the effect of dephasing in two coupled neurons with periodic oscillation [20]. Just after bifurcation, trains of spikes resulting from a noise-induced crossing over a stable manifold before reaching the node account for the clusters of dropout events observed in laser systems [19], and the ''rigid excitation'' in the Hodgkin-Huxley neuron in the presence of noise [11]. Here in coupled systems, trains of spikes also occur when coupling induces a similar early crossing over the stable manifold. We should also point out that train synchronization can also be observed in regions outside the excitable region II if the system is close to the border of homoclinic bifurcation and is *in the presence of noise*. This could be understood by the fact that the noise smears out the sharp transitions.

In excitable systems, there are separated time scales. One is determined by noise-induced escape from the well over the barrier of the potential, such as $U(x)=x^4/4-bx^3/3-x^2/2-ax$, defined in a neighborhood of the node N [19] in the system of equations (1)–(4), and the other is determined by the intrinsic dynamics of the guidance of the unstable manifold. For weak noise, the time scale for the escape from the quiescent state is long, while it is much shorter for the pulse itself. Some other mechanism can produce a similar separation of times scales. For example, in a chaotic bursting model [21] of thermally sensitive neurons, there are slow subthreshold oscillations with time scales much longer than those of the spike generation. The system can produce spike trains with chaotic pulse intervals in some temperature region. When two nonidentical chaotic neurons in such a regime are coupled, a similar transition from train synchronization to full synchronization is observed. In this model, in a certain temperature region, there is a saddle embedded in the chaotic attractor, and a homoclinic bifurcation has been identified [22] implicitly by the sudden explosion of the spike interval. Train synchronization is also observed in the vicinity of this bifurcation point. However, in this four-dimensional system, we have no knowledge of the organization of the stable and unstable manifolds, which could be very complicated [23]. Furthermore, the system trajectory visits the close neighborhood of the saddle rarely and in an intermittent way, which is different from excitable systems, where the trajectory always comes back to a stable node close to the saddle after a spike train. Thus we cannot simply ascribe the train synchronization in this system to the closeness of the stable and unstable manifolds of the saddle. In the future, it would be worthwhile to investigate synchronization under more general considerations of separated time scales in the systems.

The mechanisms for the generation of pulse trains in chaotic and excitable models of neurons are different. Similar properties of the synchronization transition and train synchronization in these classes of systems may be of importance for neurophysiology, e.g., in biological information processing. The impact of train synchronization on the behavior of networks of coupled excitable or chaotic neurons will be an interesting topic for future investigation.

ACKNOWLEDGMENTS

C.S.Z. would like to thank Professor U. Feudel for helpful discussion on the chaotic bursting model of thermally sensitive neurons. This work was supported in part by grants from the Hong Kong Research Grants Council (RGC) and the Hong Kong Baptist University Faculty Research Grant (FRG).

[1] Y. Kuramoto, *Chemical Oscillations, Waves and Turbulence* (Springer, Berlin, 1984).
[2] L. M. Pecora and T. L. Carroll, Phys. Rev. Lett. **64**, 821 (1990).
[3] N. F. Rulkov, M. M. Sushchik, L. S. Tsimring, and H. D. I. Abarbanel, Phys. Rev. E **51**, 980 (1995).
[4] M. G. Rosenblum, A. S. Pikovsky, and J. Kurths, Phys. Rev. Lett. **76**, 1804 (1996).
[5] M. G. Rosenblum, A. S. Pikovsky, and J. Kurths, Phys. Rev. Lett. **78**, 4193 (1997).
[6] A. Neiman, Phys. Rev. E **49**, 3484 (1994).
[7] B. Shulgin, A. Neiman, and V. Anishchenko, Phys. Rev. Lett. **75**, 4157 (1995).
[8] L. Gammaitoni, F. Marchesoni, and S. Santucci, Phys. Rev. Lett. **74**, 1052 (1995); A. Neiman, A. Silchenko, V. Anishchenko, and L. Schimansky-Geier, Phys. Rev. E **58**, 7118 (1998).
[9] J. F. Lindner, B. K. Meadows, W. L. Ditto, M. E. Inchiosa, and A. R. Bulsara, Phys. Rev. Lett. **75**, 3 (1995).
[10] G. Hu, T. Ditzinger, C. Z. Ning, and H. Haken, Phys. Rev.

Lett. **71**, 807 (1993); A. S. Pikovsky and J. Kurths, *ibid.* **78**, 775 (1997); A. Longtin, Phys. Rev. E **55**, 868 (1997).
[11] S. G. Lee, A. Neiman, and S. Kim, Phys. Rev. E **57**, 3292 (1998).
[12] J. L. A. Dubbeldam, B. Krauskopf, and D. Lenstra, Phys. Rev. E **60**, 6580 (1999).
[13] S. K. Han, T. G. Yim, D. E. Postnov, and O. V. Sosnovtseva, Phys. Rev. Lett. **83**, 1771 (1999).
[14] A. Neiman, L. Schimansky-Geier, A. Cornell-Bell, and F. Moss, Phys. Rev. Lett. **83**, 4896 (1999).
[15] Bambi Hu and Changsong Zhou, Phys. Rev. E **61**, R1001 (2000).
[16] T. Holten, B. Jamtveit, and P. Meakin, Geochim. Cosmochim. Acta **64**, 1893 (2000).
[17] S. Wiggins, *Global Bifurcation and Chaos* (Springer, New York, 1988).
[18] M. Giudici, C. Green, G. Giacomelli, U. Nespolo, and J. Tredicce, Phys. Rev. E **55**, 6414 (1997).
[19] A. M. Yacomotti, M. C. Eguia, J. Aliaga, O. E. Martinez, G. B. Mindlin, and A. Lipsich, Phys. Rev. Lett. **83**, 292 (1999); M. C. Eguia, G. B. Mindlin, and M. Giudici, Phys. Rev. E **58**, 2636 (1998).
[20] S. K. Han, C. Kurrer, and Y. Kuramoto, Phys. Rev. Lett. **75**, 3190 (1995); D. Postnov, S. K. Han, and H. Kook, Phys. Rev. E **60**, 2799 (1999).
[21] H. A. Braun, M. T. Huber, M. Dewald, K. Schäfer, and K. Voigt, Int. J. Bifurcation Chaos Appl. Sci. Eng. **8**, 881 (1998).
[22] U. Feudel, A. Neiman, X. Pei, W. Wojtenek, H. Braun, M. Huber, and F. Moss, Chaos **10**, 231 (2000).
[23] U. Feudel (private communication).